Editors' Suggestion

Steady-state phonon occupation of electromagnetically-induced-transparency cooling: Higher-order calculations

Shuo Zhang,[1] Tian-Ci Tian,[1] Zheng-Yang Wu,[1] Zong-Sheng Zhang,[1] Xin-Hai Wang,[1] Wei Wu,[2] Wan-Su Bao,[1,*] and Chu Guo[1,†]

[1]*Henan Key Laboratory of Quantum Information and Cryptography, Zhengzhou, Henan 450000, China*

[2]*Department of Physics, College of Liberal Arts and Sciences, National University of Defense Technology, Changsha 410073, China and China Interdisciplinary Center for Quantum Information, National University of Defense Technology, Changsha 410073, China*

(Received 6 May 2021; accepted 8 July 2021; published 28 July 2021)

Electromagnetically-induced-transparency (EIT) cooling has established itself as one of the most widely used cooling schemes for trapped ions during the past 20 years. Compared to its alternatives, EIT cooling possesses important advantages such as a tunable effective linewidth, a very low steady-state phonon occupation, and applicability for multiple ions. However, the existing analytic expression for the steady-state phonon occupation of EIT cooling is limited to the zeroth order of the Lamb-Dicke parameter. Here we extend such calculations and present the explicit expression to the second order of the Lamb-Dicke parameter. We discuss several implications of our refined formula and are able to resolve certain difficulties in existing results.

DOI: 10.1103/PhysRevA.104.013117

I. INTRODUCTION

Laser cooling of a trapped ion into its motional ground state is a key step towards various applications in quantum simulation [1–14], quantum computing [15–17], and quantum metrology [18–20], as well as testing foundations of quantum mechanics [21]. There exists a variety of cooling schemes that work in the Lamb-Dicke (LD) regime in which the Lamb-Dicke parameter η satisfies $\eta \ll 1$. Those schemes could be roughly categorized into sideband cooling [22,23], dark-state cooling [24–34], and feedback cooling [35–38].

To date, electromagnetically-induced-transparency (EIT) cooling is perhaps one of the most widely used dark-state cooling scheme in trapped-ion experiments [39–47]. Compared to its alternatives, EIT cooling possesses several outstanding advantages. First, compared to traditional sideband cooling, the resolved sideband condition, namely, the linewidth γ of the excited state should be much smaller than the axial secular trap frequency ν, is not required in EIT cooling. Second, compared to other dark-state cooling schemes as well as feedback cooling schemes, EIT cooling, in its ideal realization, only requires three internal energy levels and two static lasers, making it an experimentally friendly scheme. Third, the internal ground state is prepared as a dark state of the carrier transition, eliminating one of the two major heating mechanisms (the other one is the blue sideband transition), and therefore a very low steady-state phonon occupation could be reached. Moreover, since the internal excitation of the ion is transparent to the lasers, in a multiple ion setup, EIT cooling could easily cool down one phonon mode without heating up the others. For the same reason, it was recently pointed out that EIT cooling could actually be implemented in the strong-sideband-coupling regime, speeding up the cooling rate by more than one order of magnitude without a significant increase in the steady-state phonon occupation [48,49].

In this work we are primarily interested in the steady-state phonon occupation defined as $\bar{n}_{\rm st} = {\rm tr}(\hat{n}\hat{\rho}_{\rm st})$, where $\hat{n}$ is the phonon number operator and $\hat{\rho}_{\rm st}$ is the density operator of the system at steady state. In the literature, $\bar{n}_{\rm st}$ is often expressed as an η-independent term plus a contribution of the order η^2, that is, $\bar{n}_{\rm st} = {\rm const} + O(\eta^2)$. Here we note that the recoil energy due to one-photon emission is of the order η^2. As an example, for sideband cooling $\bar{n}_{\rm st}^{\rm sb} = (\alpha + \frac{1}{4})(\frac{\gamma}{2\nu})^2 + O(\eta^2)$, where the geometry factor $\alpha = \frac{2}{5}$ for the dipole transition, while for standing-wave sideband cooling $\bar{n}_{\rm st}^{\rm SWSC} = \frac{1}{4}(\frac{\gamma}{2\nu})^2 + O(\eta^2)$ [50]. In comparison, $\bar{n}_{\rm st}^{\rm EIT}$ for EIT cooling was first given in Ref. [24] as

$$\bar{n}_{\rm st}^{\rm EIT} = \frac{\gamma^2}{16\Delta^2} + O(\eta^2), \tag{1}$$

where Δ is the detuning for both lasers used in EIT cooling. Equation (1) also reflects the flexibility of EIT cooling since Δ is highly tunable, while in the case of sideband cooling, the axial secular trap frequency ν is often a given constant. Subsequent dark-state cooling schemes utilize more complicated energy-level structures and laser setups to suppress both the carrier and blue sideband transitions, thus completely eliminating the η-independent term on the right-hand side of Eq. (1) and reaching a steady-state phonon occupation of $O(\eta^2)$ [25,27–29,34], which means that the ion could be cooled down to recoil or even subrecoil temperature.

To this end we point out that the expression (1) poses at least two theoretical difficulties. (i) In the EIT cooling setup, the excited state $|e\rangle$ of linewidth γ dissipates to two ground states $|g\rangle$ and $|r\rangle$, with dissipation rates γ_g and γ_r satisfying

*bws@qiclab.cn
†guochu604b@gmail.com

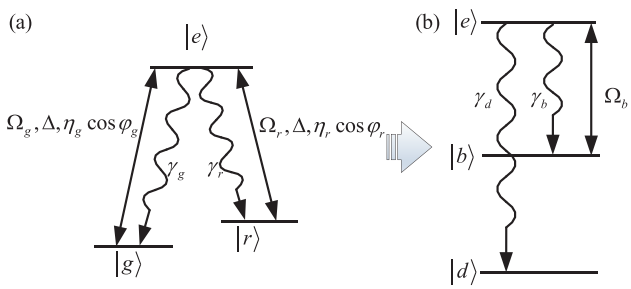

FIG. 1. (a) Standard three-level configuration of EIT cooling. The system consists of a dissipative excited state $|e\rangle$ and two ground states $|g\rangle$ and $|r\rangle$. The transitions $|e\rangle \leftrightarrow |g\rangle$ and $|e\rangle \leftrightarrow |r\rangle$ are induced by two external lasers. (b) Dynamics of internal degrees of freedom can be understood on the basis of $\{|e\rangle, |b\rangle, |d\rangle\}$, where the dark state $|d\rangle$ decouples from $|b\rangle$ and $|e\rangle$, and the bright state $|b\rangle$ is coupled to $|e\rangle$ with an effective coupling strength Ω_b.

$\gamma = \gamma_g + \gamma_r$, as can be seen from Fig. 1(a). However, the dark state is a certain combination of $|g\rangle$ and $|r\rangle$, and cooling is essentially induced by an effective dissipation rate γ_{eff} from $|e\rangle$ to this dark state. In a certain parameter regime (which does not violates the EIT cooling conditions) one could even have $\gamma_{\text{eff}} \approx 0$ (this statement will become clear later) and cooling should not be possible. Such an effect cannot be predicted from Eq. (1) since it only depends on γ. (ii) The detuning Δ is usually highly tunable in experiments. Therefore, it is possible to make it very large such that $\frac{\gamma^2}{16\Delta^2}$ is comparable to or even less than the $O(\eta^2)$ term, in which case the recoil temperature could already be achieved without eliminating the blue sideband. However, this statement can only be made precise once we have the exact expression for the $O(\eta^2)$ term. Therefore, in this work we perform a more refined calculation of $\bar{n}_{\text{st}}^{\text{EIT}}$ which gives us an explicit expression to the order of η^2, with which we are able to resolve these two difficulties.

This paper is organized as follows. In Sec. II we derive the master equation for EIT cooling in a slightly different representation compared to previous works, which would be more convenient for the derivations in this work. In Sec. III we solve the master equation to obtain our main result, namely, the analytic expression for the $O(\eta^2)$ term in Eq. (1). We verify our result by comparing it with the exact numerical solutions of the master equation. We also discuss several implications of it and use it to resolve the two above-mentioned difficulties of Eq. (1). We summarize in Sec. IV. Since in this work we focus on only EIT cooling, we will eliminate the superscript in the expression of $\bar{n}_{\text{st}}^{\text{EIT}}$ in the following.

II. MASTER EQUATION FOR EIT COOLING

In a standard EIT cooling setup, an ion of mass M is confined in a harmonic trap with axial secular trap frequency ν. As shown in Fig. 1(a), the excited state $|e\rangle$ is coupled to two ground states $|g\rangle$ and $|r\rangle$ by two lasers with frequencies ω_g and ω_r and with Rabi frequencies Ω_g and Ω_r. The angles of the lasers with respect to the motional axis are φ_g and φ_r, respectively. The excited state $|e\rangle$ dissipates to $|g\rangle$ and $|r\rangle$ with rates γ_g and γ_r. The energy differences between $|e\rangle$ and $|g\rangle$ and between $|e\rangle$ and $|r\rangle$ are denoted by Δ_{eg} and Δ_{er}, respectively.

The dynamics of the system is described by the Lindblad master equation [51,52] (we set $\hbar = 1$ throughout this work)

$$\frac{d}{dt}\hat{\rho}(t) = -i[\hat{H}, \hat{\rho}(t)] + \mathcal{D}(\hat{\rho}(t)). \tag{2}$$

Here $\hat{\rho}(t)$ is the density operator of the system at time t. The Hamiltonian $\hat{H}$ takes the form

$$\begin{aligned}\hat{H} &= \nu\hat{a}^\dagger\hat{a} - \Delta|e\rangle\langle e| \\ &\quad + \left(\frac{\Omega_g}{2}|e\rangle\langle g|e^{ik_g\hat{x}\cos(\varphi_g)} + \text{H.c.}\right) \\ &\quad + \left(\frac{\Omega_r}{2}|e\rangle\langle r|e^{ik_r\hat{x}\cos(\varphi_r)} + \text{H.c.}\right),\end{aligned} \tag{3}$$

where $\hat{a}^\dagger$ ($\hat{a}$) is the creation (annihilation) operator of the ion's motional state (phonon), $\hat{x} = \frac{1}{\sqrt{2M\nu}}(\hat{a}^\dagger + \hat{a})$ is the position operator, and the wave numbers $k_g = \omega_g/c$ and $k_r = \omega_r/c$ (c is the speed of light). As one of the EIT cooling conditions, the detunings of both lasers are tuned to the same, that is,

$$\Delta = \omega_g - \Delta_{eg} = \omega_r - \Delta_{er}. \tag{4}$$

The LD parameters η_g and η_r related to the two lasers are defined as

$$\eta_g = k_g\sqrt{\frac{1}{2M\nu}}, \quad \eta_r = k_r\sqrt{\frac{1}{2M\nu}}. \tag{5}$$

Expanding $\hat{H}$ to the first order of η_g and η_r, we get

$$\begin{aligned}\hat{H}_{\text{LD}} &= \nu\hat{a}^\dagger\hat{a} - \Delta|e\rangle\langle e| \\ &\quad + \left(\frac{\Omega_g}{2}|e\rangle\langle g| + \frac{\Omega_r}{2}|e\rangle\langle r| + \text{H.c.}\right) \\ &\quad + \left(i\eta_g\cos(\varphi_g)\frac{\Omega_g}{2}|e\rangle\langle g|(\hat{a}^\dagger + \hat{a}) + \text{H.c.}\right) \\ &\quad + \left(i\eta_r\cos(\varphi_r)\frac{\Omega_r}{2}|e\rangle\langle r|(\hat{a}^\dagger + \hat{a}) + \text{H.c.}\right).\end{aligned} \tag{6}$$

The dissipative part $\mathcal{D}$ will only be kept to the zeroth order of the LD parameters since the next nonvanishing term would contribute only to the fourth order of the LD parameters [50], namely, we take $\mathcal{D} \approx \mathcal{D}_0$, with

$$\mathcal{D}_0(\hat{\rho}) = \sum_{j=g,r}\frac{\gamma_j}{2}(2|j\rangle\langle e|\hat{\rho}|e\rangle\langle j| - \{\hat{\rho}, |e\rangle\langle e|\}). \tag{7}$$

We note that $\mathcal{D}_0$ denotes the usual spontaneous emission when the atomic motion is neglected.

Under the condition (4), we can perform a unitary transformation on the subspace $\{|g\rangle, |r\rangle\}$ spanned by states $|g\rangle$ and $|r\rangle$ as

$$|d\rangle = \cos(\theta)|g\rangle - \sin(\theta)|r\rangle, \tag{8}$$

$$|b\rangle = \sin(\theta)|g\rangle + \cos(\theta)|r\rangle, \tag{9}$$

with $\tan(\theta) = \Omega_g/\Omega_r$. Then $|d\rangle$ is a dark state in that it decouples from the subspace spanned by $|b\rangle$ and $|e\rangle$ if only the internal degrees of freedom are considered. Here $|b\rangle$ is referred to as the bright state since it is coupled to $|e\rangle$. In the usual derivation of EIT cooling, $|b\rangle$ and $|e\rangle$ are further

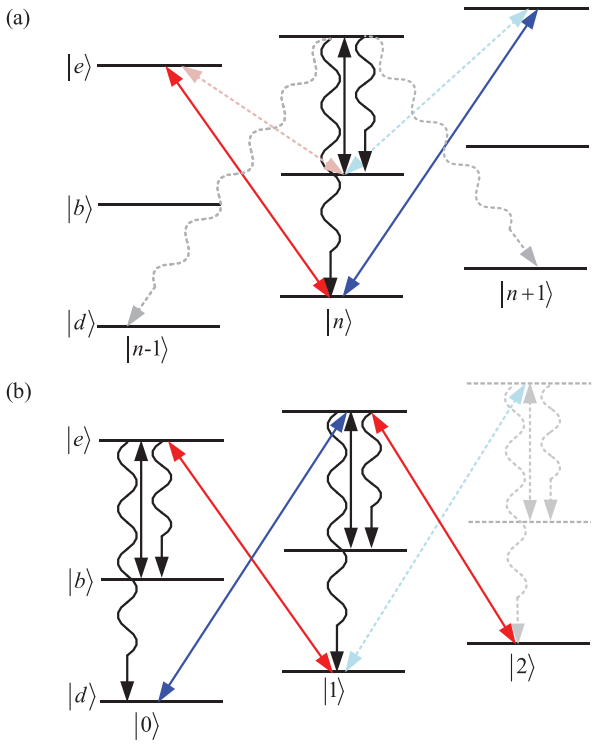

FIG. 2. The EIT cooling dynamics in the $\{|d\rangle, |b\rangle, |e\rangle\}$ representation. (a) All the possible transitions up to η^2 are shown by solid lines, which include $|d,n\rangle \leftrightarrow |e,n\pm 1\rangle$, $|b,n\rangle \leftrightarrow |e,n\rangle$, and dissipations $|e,n\rangle \to |b,n\rangle$ and $|e,n\rangle \to |d,n\rangle$. Meanwhile, the contributions of the sideband transitions $|b,n\rangle \leftrightarrow |e,n\pm 1\rangle$ as well as the effective dissipations $|e,n\rangle \to |d,n\pm 1\rangle$ are of $O(\eta^4)$ and are shown by dashed lines. (b) In the steady state of EIT cooling, the population is mostly in the state $|d,0\rangle$. We thus are limited to the subspace $\mathcal{V}_0$ spanned by the seven energy levels most closely related to this state as shown by the solid lines.

diagonalized into two states $|\pm\rangle$ such that the internal degrees of freedom are fully diagonalized. The second condition for EIT cooling is chosen as

$$\Delta = \frac{\Omega_g^2 + \Omega_r^2}{4\nu} \tag{10}$$

such that the red sideband transition $|d,n+1\rangle \leftrightarrow |+,n\rangle$ is resonant [24,53]. In the $\{|d\rangle, |\pm\rangle\}$ representation, the state $|-\rangle$ is neglected since it is far off-resonance, leaving the two states $\{|d\rangle, |+\rangle\}$ together with the phonon states closely resembling the standing-wave sideband cooling [48], with an effective dissipation rate from $|+\rangle$ to $|d\rangle$ denoted by $\gamma_{\rm eff}$. In general, $\gamma_{\rm eff} < \gamma$. This physical picture, although nice for a rough understanding since it reduces the model to the well-understood standing-wave sideband cooling, has one important difficulty that if we directly apply the standing-wave sideband cooling formalism, the obtained $\bar{n}_{\rm st}$ will only depend on $\gamma_{\rm eff}$ instead of γ. The truth is that the dynamics between $|d\rangle$ and $|-\rangle$ cannot really be neglected since the internal dynamics in the subspace $\{|b\rangle, |e\rangle\}$ could still be much faster than that of the red sideband. To correctly obtain a refined expression for $\bar{n}_{\rm st}$, one has to take all the internal states into account. We thus work in the $\{|d\rangle, |b\rangle, |e\rangle\}$ representation of the internal states in the following, which is shown in Fig. 2(a). In this representation we can rewrite $\hat{H}_{\rm LD}$ in Eq. (6) as

$$\hat{H}_{\rm LD} = \nu\hat{a}^\dagger\hat{a} - \Delta|e\rangle\langle e| + \left(\frac{\Omega_b}{2}|e\rangle\langle b| + {\rm H.c.}\right) + \left(i\eta\frac{\Omega_d}{2}|e\rangle\langle d|(\hat{a}+\hat{a}^\dagger) + {\rm H.c.}\right), \tag{11}$$

where $\Omega_d = \frac{\Omega_g\Omega_r}{\sqrt{\Omega_g^2+\Omega_r^2}}$, $\Omega_b = \sqrt{\Omega_g^2+\Omega_r^2}$, and $\eta = \eta_g\cos(\varphi_g) - \eta_r\cos(\varphi_r)$. Here we have neglected the sideband transitions between $|b,n\rangle$ and $|e,n\pm 1\rangle$ since their contributions are of the order η^4. We can also rewrite $\mathcal{D}_0$ in Eq. (7) as

$$\mathcal{D}_0(\hat{\rho}) = \sum_{j=d,b}\frac{\gamma_j}{2}(2|j\rangle\langle e|\hat{\rho}|e\rangle\langle j| - \{\hat{\rho}, |e\rangle\langle e|\}), \tag{12}$$

with $\gamma_d = \gamma_g\cos^2(\theta) + \gamma_r\sin^2(\theta)$ and $\gamma_b = \gamma_r\cos^2(\theta) + \gamma_g\sin^2(\theta)$.

III. RESULTS AND DISCUSSION

In the following we compute the steady-state solution of Eq. (2) to the second order of η. Since the population is mostly in the state $|d,0\rangle$ when reaching the steady state of EIT cooling, we restrict Eq. (2) to the subspace $\mathcal{V}_0$ spanned by the seven states

$$\mathcal{V}_0 = \{|d,0\rangle, |b,0\rangle, |e,0\rangle, |d,1\rangle, |b,1\rangle, |e,1\rangle, |d,2\rangle\}, \tag{13}$$

as shown in Fig. 2(b). The reason for this choice is that the states in $\mathcal{V}_0$ can be reached by at most one blue sideband transition starting from $|d,0\rangle$, which is assumed to be much weaker than both the dissipation and the red sideband. Then the steady-state solution $\hat{\rho}_{\rm st}$ to Eq. (2) in the subspace $\mathcal{V}_0$ can be found by solving the set of equations

$${\rm tr}(\hat{O}\mathcal{P}\{-i[\hat{H}_{\rm LD}, \hat{\rho}_{\rm st}] + \mathcal{D}_0(\hat{\rho}_{\rm st})\}) = 0, \tag{14}$$

where $\mathcal{P}$ is the projection operator into the subspace $\mathcal{V}_0$ and $\hat{O}$ is an operator belonging to the group $\{|j\rangle\langle j|, |j\rangle\langle k| + |k\rangle\langle j|, i|j\rangle\langle k| - i|k\rangle\langle j|\}$ $(j \neq k)$, where $|j\rangle$ and $|k\rangle$ are any of the states in $\mathcal{V}_0$.

Equation (14) contains 49 equations in total, which in general is not easy to solve directly. However, under the conditions $\gamma_g, \gamma_r \ll \Delta$, $\eta\Omega_d \ll \Omega_b$, and Eq. (10), we find that certain subblock of equations decouples from the rest, thus simplifying the calculations, and we can get the solutions for all the diagonal terms as

$$\rho_{b0,b0} = \frac{\eta^2\Omega_d^2(\gamma_d+\gamma_b)}{4\Omega_b^2\gamma_d}\rho_{d0,d0}, \tag{15a}$$

$$\rho_{e0,e0} = 0, \tag{15b}$$

$$\rho_{d1,d1} = \frac{\eta^2\Omega_d^2(\gamma_d+\gamma_b)}{4\Omega_b^2\gamma_d}\left(1 + \frac{4\gamma_d\nu^2(\gamma_d+\gamma_b)}{\eta^2\Omega_d^2\Omega_b^2}\right)\rho_{d0,d0}, \tag{15c}$$

$$\rho_{b1,b1} = \frac{\eta^2\Omega_d^2(\gamma_d+\gamma_b)}{4\Omega_b^2\gamma_d}\rho_{d0,d0}, \tag{15d}$$

$$\rho_{e1,e1} = 0, \tag{15e}$$

$$\rho_{d2,d2} = \frac{\eta^2\Omega_d^2}{4\Omega_b^2}\left(\frac{\gamma_b}{\gamma_d}\right)\rho_{d0,d0}. \tag{15f}$$

Here we have used $\rho_{b0,b0} = \mathrm{tr}(|b,0\rangle\langle b,0|\mathcal{P}\rho)$ and similar solutions for other terms. The detailed derivation of Eq. (15) is in the Appendix. Using $\rho_{d0,d0} \approx 1$, we obtain $\bar{n}_{\mathrm{st}}$ as

$$\begin{aligned}\bar{n}_{\mathrm{st}} &\approx \rho_{d1,d1} + \rho_{b1,b1} + \rho_{e1,e1} + 2\rho_{d2,d2} \\ &\approx \frac{\gamma^2}{16\Delta^2} + \frac{\eta^2\Omega_d^2}{\Omega_b^2}\left(\frac{1}{2} + \frac{\gamma_b}{\gamma_d}\right).\end{aligned} \tag{16}$$

Equation (16) is the main result of this work. Compared with Eq. (1), we can see that it gives the explicit expression to the order of η^2. In the following we discuss two special parameter regimes which are frequently considered.

First, $\Omega_g \ll \Omega_r$ and thus $\theta \approx 0$. In this regime we have $|d\rangle \approx |g\rangle$, $|b\rangle \approx |r\rangle$, $\Omega_d \approx \Omega_g$, $\Omega_b \approx \Omega_r$, $\gamma_d \approx \gamma_g$, and $\gamma_b \approx \gamma_r$. Consequently, we have

$$\bar{n}_{\mathrm{st}} \approx \frac{\gamma^2}{16\Delta^2} + \frac{\eta^2\Omega_g^2}{\Omega_r^2}\left(\frac{1}{2} + \frac{\gamma_r}{\gamma_g}\right). \tag{17}$$

In the usual experimental setup, the condition $\gamma_g \geqslant \gamma_r$ can be satisfied (if this is not satisfied, one could simply swap the roles of $|g\rangle$ and $|r\rangle$). In this case the coefficient of the η^2 term on the right-hand side of Eq. (17) can often be smaller compared to the first term and then Eq. (1) will agree well with the exact solution of Eq. (2). Now we note that in Eq. (17), the η^2 term is explicitly dependent on γ_g and γ_r. From a purely theoretical point of view, Eq. (17) shows that $\bar{n}_{\mathrm{st}}$ diverges when $\gamma_g \to 0$, which coincides with the intuition that in this limit ground-state cooling cannot be achieved. This is an effect which cannot be predicted from Eq. (1).

Second, $\Omega_g = \Omega_r$ and thus $\theta = \pi/4$. In this case $|d\rangle$ and $|b\rangle$ are equal superpositions of states $|g\rangle$ and $|r\rangle$ as $|d\rangle = \frac{1}{\sqrt{2}}(|g\rangle + |r\rangle)$ and $|b\rangle = \frac{1}{\sqrt{2}}(|g\rangle - |r\rangle)$, and $\Omega_d = \frac{\Omega_b}{2} = \frac{1}{\sqrt{2}}\Omega_r$ and $\gamma_d = \gamma_b = \frac{\gamma}{2}$. Thus we have

$$\bar{n}_{\mathrm{st}} \approx \frac{\gamma^2}{16\Delta^2} + \frac{3}{8}\eta^2. \tag{18}$$

From Eqs. (17) and (18) we can see that for EIT cooling, the contribution from the η^2 term is not necessarily smaller than from the η-independent term, since we can tune Δ to be much larger than γ with the EIT cooling conditions in Eqs. (4) and (10) still being satisfied. The necessity of using more elaborate dark-state cooling schemes with more lasers is thus obscure since one could already reach the recoil temperature with carefully tuned parameters in standard EIT cooling. To this end, the two difficulties from Eq. (1) have been resolved based on our analytical result.

To verify Eq. (16), we compare it with the exact numerical solution of Eq. (2), which is shown in Fig. 3. To clearly see the effect of the η^2 term in Eq. (16), we also plot in Fig. 3 the predictions from Eq. (1) without the η^2 correction term. More concretely, we perform two sets of simulations, one with $\Omega_g = \Omega_r/5$ [Figs. 3(a), 3(c), and 3(e)] and the other with $\Omega_g = \Omega_r$ [Figs. 3(b), 3(d), and 3(f)]. In each set of simulations, we show $\bar{n}_{\mathrm{st}}$ as a function of Ω_g [Figs. 3(a) and 3(b)], η_g [Figs. 3(c) and 3(d)], and γ_g [Figs. 3(e) and 3(f)], respectively. We can see

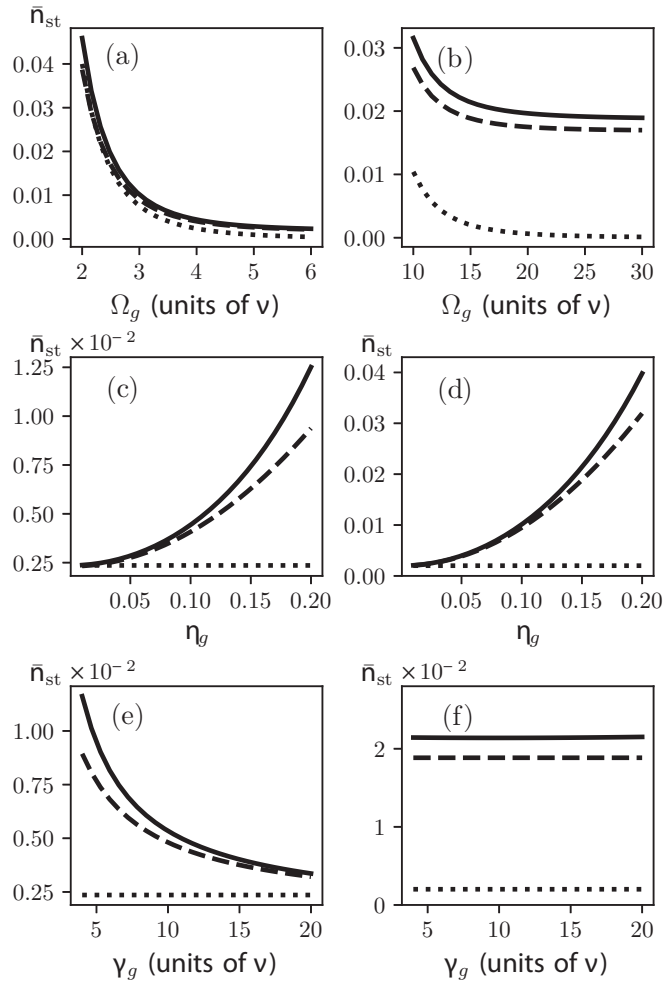

FIG. 3. Comparison of predicted steady-state phonon occupation $\bar{n}_{\mathrm{st}}$. The solid, dashed, and dotted lines in all the panels stand for the exact numerical solutions from Eq. (2), predictions from our analytical expression (16), and predictions from the previous results in Eq. (1) with the $O(\eta^2)$ term neglected, respectively. (a), (c), and (e) Plot of $\bar{n}_{\mathrm{st}}$ as a function of (a) Ω_g, (c) η_g, and (e) γ_g, under the condition $\Omega_g = \Omega_r/5$. (b), (d), and (f) Plot of $\bar{n}_{\mathrm{st}}$ as a function of (b) Ω_g, (d) η_g, and (e) γ_g, under the condition $\Omega_g = \Omega_r$. In (c) and (e) we have used $\Omega_g = 4\nu$, while in (d) and (f) we have used $\Omega_g = 15\nu$. In (e) and (f) we have set $\gamma_g + \gamma_r = 20\nu$. The other parameters (if not specified in the figures) are $\gamma_g/\nu = 20/3$, $\gamma_r/\nu = 40/3$, $\eta_g = \eta_r = 0.15$, $\varphi_g = \pi/4$, and $\varphi_r = 3\pi/4$; Δ is chosen according to Eq. (10).

that in all the panels predictions from our analytical expression (16) agree better with the exact numerical solutions. In particular, from Figs. 3(b), 3(d), and 3(f) we can see that the effect of the η^2 term is more significant when $\Omega_g = \Omega_r$; this is because in this case the Ω_d/Ω_r term in the coefficient of η^2 reaches its maximum value $\frac{1}{2}$. From Figs. 3(c) and 3(d) we can see that the η^2 correction term is more significant when η_g becomes larger; in fact, it can be several times larger than the contribution of the zeroth term in Eq. (1) when η_g approaches a moderate value of 0.2. Figure 3(e) also reveals the failure of Eq. (1) when $\Omega_g \ll \Omega_r$ and γ_g is small, which is the case

we considered in Eq. (17). Figure 3(f) demonstrates the case of Eq. (18), where our prediction differs from Eq. (1) by a constant shift $3\eta^2/8$, and we can see that this shift could be much larger than the zeroth-order term $\frac{\gamma^2}{16\Delta^2}$.

The parameter regimes considered in our numerical simulations could readily be explored in current ion cooling experiments. Taking the $^{40}Ca^+$ ion as an example, EIT cooling can be implemented on the $^2S_{1/2} \to {}^2P_{1/2}$ transition. Both $^2S_{1/2}$ and $^2P_{1/2}$ have two Zeeman sublevels, which constitute a four-level system. Then one can choose either $|e\rangle = |P,+\rangle$, $|g\rangle = |S,+\rangle$, and $|r\rangle = |S,-\rangle$ or $|e\rangle = |P,-\rangle$, $|g\rangle = |S,-\rangle$, and $|r\rangle = |S,+\rangle$ for EIT cooling. For both choices we have $\gamma_g/\gamma_r = 1/2$, which is the case we considered in Figs. 3(a)–3(d). The Rabi frequencies Ω_g and Ω_r vary case by case; however, from Eq. (16) we can see that what really matters for $\bar{n}_{\rm st}$ is the ratio Ω_g/Ω_r, which is often widely tunable in experiments. The Lamb-Dicke parameter could be tuned by changing the relative angle between lasers or using different ions (for example, the Be^+ and Yb^+ ions have very different masses and thus the Lamb-Dicke parameters will be very different if the laser angle remains the same [44–46]). Here we also note that for a very large Lamb-Dicke parameter, Eqs. (1) and (16) would no longer be valid. This situation is studied numerically in Ref. [54]. The ratio γ_g/γ_r can be tuned by using different ions; for example, for Yb^+ we have $\gamma_g/\gamma_r = 1$ [45]. The numerical solutions of the Lindblad master equation are obtained using the QUTIP package [55].

IV. CONCLUSION

In summary, we have derived a refined expression for the steady-state phonon occupation $\bar{n}_{\rm st}$ of the EIT cooling, where the contribution to the second order of the Lamb-Dicke parameter was explicitly given. Based on our analytical result, we showed that $\bar{n}_{\rm st}$ not only depends on the linewidth γ of the excited state, but also depends on the detailed ratios Ω_d/Ω_b and γ_b/γ_d. In particular, we pointed out that if $\Omega_g \ll \Omega_r$, then $\bar{n}_{\rm st}$ diverges when $\gamma_g \to 0$, thus resolving one difficulty from Eq. (1) which predicts that $\bar{n}_{\rm st} \to 0$ even in a parameter regime that cooling cannot be achieved. We also showed that the η^2 correction term may well be larger than the η-independent term when $\Omega_g \approx \Omega_r$ or when η_g is large, which means that with standard EIT cooling one could already reach the recoil temperature, obscuring the necessity of utilizing more complicated dark-state cooling schemes. Our results indicate that to suppress the η^2 correction term, thus reaching a low steady-state phonon occupation in ion cooling experiments, one should properly choose the energy levels as well as the laser strengths such that $\Omega_g \ll \Omega_r$ and that γ_g is comparable to or larger than γ_r.

ACKNOWLEDGMENTS

We thank Jie Zhang for fruitful discussion. C.G. acknowledges support from National Natural Science Foundation of China through Grant No. 11805279. W.W. acknowledges support from National Basic Research Program of China through Grant No. 2016YFA0301903.

APPENDIX: DETAILS FOR DERIVING THE STEADY-STATE PHONON OCCUPATION

We denote the Hamiltonian $\hat{H}_{\rm LD}$ and $\mathcal{D}$ in the subspace $\mathcal{V}_0$ by $\hat{H}^s_{\rm LD}$ and $\mathcal{D}^s$, which can be written as

$$\begin{aligned}\hat{H}^s_{\rm LD} =& -\Delta|e,0\rangle\langle e,0| + \nu|d,1\rangle\langle d,1| + \nu|b,1\rangle\langle b,1| \\ &- (\Delta-\nu)|e,1\rangle\langle e,1| + 2\nu|d,2\rangle\langle d,2| \\ &+ \frac{\Omega_b}{2}(|b,0\rangle\langle e,0| + |e,0\rangle\langle b,0|) \\ &+ \frac{\Omega_b}{2}(|b,1\rangle\langle e,1| + |e,1\rangle\langle b,1|) \\ &+ i\frac{\eta\Omega_d}{2}(|e,1\rangle\langle d,0| - |g,0\rangle\langle e,1|) \\ &+ i\frac{\eta\Omega_d}{2}(|e,0\rangle\langle d,1| - |d,1\rangle\langle e,0|) \\ &+ i\frac{\eta\Omega_d}{2}(|e,1\rangle\langle d,2| - |d,2\rangle\langle e,1|) \end{aligned} \tag{A1}$$

and

$$\begin{aligned}\mathcal{D}^s(\hat{\rho}) =& \frac{\gamma_d}{2}(2|d,0\rangle\langle e,0|\hat{\rho}|e,0\rangle\langle d,0| - \{\hat{\rho}, |e,0\rangle\langle e,0|\}) \\ &+ \frac{\gamma_d}{2}(2|d,1\rangle\langle e,1|\hat{\rho}|e,1\rangle\langle d,1| - \{\hat{\rho}, |e,1\rangle\langle e,1|\}) \\ &+ \frac{\gamma_b}{2}(2|b,0\rangle\langle e,0|\hat{\rho}|e,0\rangle\langle b,0| - \{\hat{\rho}, |e,0\rangle\langle e,0|\}) \\ &+ \frac{\gamma_b}{2}(2|b,1\rangle\langle e,1|\hat{\rho}|e,1\rangle\langle b,1| - \{\hat{\rho}, |e,1\rangle\langle e,1|\}), \end{aligned} \tag{A2}$$

respectively. Substituting Eqs. (A1) and (A2) and all the possible $\hat{O}$ into Eq. (14), we will get 49 coupled equations. Here we first consider the seven equations by taking $\hat{O} = |j\rangle\langle j|$, which are

$$\gamma_d\rho_{e0,e0} - \frac{\eta\Omega_d}{2}\sigma^x_{d0,e1} = 0, \tag{A3}$$

$$\gamma_b\rho_{e0,e0} - \frac{\Omega_b}{2}\sigma^y_{b0,e0} = 0, \tag{A4}$$

$$-(\gamma_d+\gamma_b)\rho_{e0,e0} + \frac{\Omega_b}{2}\sigma^y_{b0,e0} + \frac{\eta\Omega_d}{2}\sigma^x_{e0,d1} = 0, \tag{A5}$$

$$\gamma_d\rho_{e1,e1} - \frac{\eta\Omega_d}{2}\sigma^x_{e0,d1} = 0, \tag{A6}$$

$$\gamma_b\rho_{e1,e1} - \frac{\Omega_b}{2}\sigma^y_{b1,e1} = 0, \tag{A7}$$

$$\begin{aligned}&-(\gamma_d+\gamma_b)\rho_{e1,e1} + \frac{\eta\Omega_d}{2}\sigma^x_{d0,e1} \\ &+ \frac{\Omega_b}{2}\sigma^y_{b1,e1} + \frac{\eta\Omega_d}{2}\sigma^x_{e1,d2} = 0,\end{aligned} \tag{A8}$$

$$-\frac{\eta\Omega_d}{2}\sigma^x_{e1,d2} = 0, \tag{A9}$$

where we have used $\sigma^y_{jk} = {\rm tr}[(i|j\rangle\langle k| - i|k\rangle\langle j|)\hat{\rho}_{\rm st}]$ and $\sigma^x_{jk} = {\rm tr}[(|j\rangle\langle k| + |k\rangle\langle j|)\hat{\rho}_{\rm st}]$. Solving the above equations, we get

$$\rho_{e0,e0} = \rho_{e1,e1}, \tag{A10a}$$

$$\sigma^x_{d0,e1} = \sigma^x_{e0,d1}, \tag{A10b}$$

$$\sigma^y_{b0,e0} = \sigma^y_{b1,e1}. \tag{A10c}$$

Now we substitute Eqs. (A10) into the eight equations

$$\gamma_b \rho_{e0,e0} - \frac{\Omega_b}{2}\sigma^y_{b0,e0} = 0, \tag{A11}$$

$$\gamma_d \rho_{e1,e1} - \frac{\eta\Omega_d}{2}\sigma^x_{e0,d1} = 0, \tag{A12}$$

$$-\frac{\gamma_d+\gamma_b}{2}\sigma^x_{b0,e0} + \Delta\sigma^y_{b0,e0} + \frac{\eta\Omega_d}{2}\sigma^x_{b0,d1} = 0, \tag{A13}$$

$$-\Omega_b\rho_{e0,e0} - \Delta\sigma^x_{b0,e0} - \frac{\gamma_b+\gamma_d}{2}\sigma^y_{b0,e0} + \frac{\eta\Omega_d}{2}\sigma^y_{b0,d1} + \Omega_b\rho_{b0,b0} = 0, \tag{A14}$$

$$-\frac{\eta\Omega_d}{2}\sigma^x_{b0,e0} - \nu\sigma^y_{b0,d1} + \frac{\Omega_b}{2}\sigma^y_{e0,d1} = 0, \tag{A15}$$

$$-\frac{\eta\Omega_d}{2}\sigma^y_{b0,e0} + \nu\sigma^x_{b0,d1} - \frac{\Omega_b}{2}\sigma^x_{e0,d1} = 0, \tag{A16}$$

$$-\eta\Omega_d\rho_{e0,e0} + \eta\Omega_d\rho_{d1,d1} + \frac{\Omega_b}{2}\sigma^y_{b0,d1} - \frac{\gamma_d+\gamma_b}{2}\sigma^x_{e0,d1} - (\nu+\Delta)\sigma^y_{e0,d1} = 0, \tag{A17}$$

$$-\frac{\Omega_b}{2}\sigma^x_{b0,d1} + (\nu+\Delta)\sigma^x_{e0,d1} - \frac{\gamma_b+\gamma_d}{2}\sigma^y_{e0,d1} = 0, \tag{A18}$$

which, together with the conditions $4\Delta\nu = \Omega_b^2$ and $\eta^2\Omega_d^2 \ll \Omega_b^2$, result in

$$\rho_{d1,d1} \approx \rho_{b0,b0}\left(1 + \frac{4\gamma_d\nu^2(\gamma_d+\gamma_b)}{\eta^2\Omega_d^2\Omega_b^2}\right), \tag{A19}$$

$$\sigma^x_{d0,e1} = \sigma^x_{e0,d1} \approx \rho_{b0,b0}\frac{8\nu^2\gamma_d}{\eta\Omega_d\Omega_b^2}, \tag{A20}$$

$$\sigma^y_{b1,e1} = \sigma^y_{b0,e0} \approx \rho_{b0,b0}\frac{8\nu^2\gamma_b}{\Omega_b^3}. \tag{A21}$$

Now substituting $\sigma^x_{d0,e1}$, $\sigma^x_{e0,d1}$, $\sigma^y_{b1,e1}$, and $\sigma^y_{b0,e0}$ back into Eq. (14), we get the solutions [Eq. (15)] for the diagonal terms.

[1] D. Porras and J. I. Cirac, Phys. Rev. Lett. **92**, 207901 (2004).
[2] D. Porras and J. I. Cirac, Phys. Rev. Lett. **93**, 263602 (2004).
[3] D. Leibfried, R. Blatt, C. Monroe, and D. Wineland, Rev. Mod. Phys. **75**, 281 (2003).
[4] A. Bermúdez, M. Bruderer, and M. B. Plenio, Phys. Rev. Lett. **111**, 040601 (2013).
[5] A. Ruiz, D. Alonso, M. B. Plenio, and A. del Campo, Phys. Rev. B **89**, 214305 (2014).
[6] M. Ramm, T. Pruttivarasin, and H. Häffner, New J. Phys. **16**, 063062 (2014).
[7] C. Guo, M. Mukherjee, and D. Poletti, Phys. Rev. A **92**, 023637 (2015).
[8] C. Guo and D. Poletti, Phys. Rev. A **94**, 033610 (2016).
[9] C. Guo and D. Poletti, Phys. Rev. A **95**, 052107 (2017).
[10] C. Guo and D. Poletti, Phys. Rev. B **96**, 165409 (2017).
[11] C. Guo and D. Poletti, Phys. Rev. A **98**, 052126 (2018).
[12] X. Xu, J. Thingna, C. Guo, and D. Poletti, Phys. Rev. A **99**, 012106 (2019).
[13] Y. Pan, J. Zhang, E. Cohen, C.-W. Wu, P.-X. Chen, and N. Davidson, Nat. Phys. **16**, 1206 (2020).
[14] C.-W. Wu, J. Zhang, Y. Xie, B.-Q. Ou, T. Chen, W. Wu, and P.-X. Chen, Phys. Rev. A **100**, 062111 (2019).
[15] J. I. Cirac and P. Zoller, Phys. Rev. Lett. **74**, 4091 (1995).
[16] B. P. Lanyon, C. Hempel, D. Nigg, M. Müller, R. Gerritsma, F. Zähringer, P. Schindler, J. T. Barreiro, M. Rambach, G. Kirchmair *et al.*, Science **334**, 57 (2011).
[17] D. Kielpinski, C. Monroe, and D. J. Wineland, Nature (London) **417**, 709 (2002).
[18] C.-W. Chou, D. B. Hume, J. C. J. Koelemeij, D. J. Wineland, and T. Rosenband, Phys. Rev. Lett. **104**, 070802 (2010).
[19] A. D. Ludlow, M. M. Boyd, J. Ye, E. Peik, and P. O. Schmidt, Rev. Mod. Phys. **87**, 637 (2015).
[20] N. Huntemann, C. Sanner, B. Lipphardt, C. Tamm, and E. Peik, Phys. Rev. Lett. **116**, 063001 (2016).
[21] D. J. Wineland, Rev. Mod. Phys. **85**, 1103 (2013).
[22] C. Monroe, D. M. Meekhof, B. E. King, S. R. Jefferts, W. M. Itano, D. J. Wineland, and P. Gould, Phys. Rev. Lett. **75**, 4011 (1995).
[23] C. Roos, T. Zeiger, H. Rohde, H. C. Nägerl, J. Eschner, D. Leibfried, F. Schmidt-Kaler, and R. Blatt, Phys. Rev. Lett. **83**, 4713 (1999).
[24] G. Morigi, J. Eschner, and C. H. Keitel, Phys. Rev. Lett. **85**, 4458 (2000).
[25] J. Evers and C. H. Keitel, Europhys. Lett. **68**, 370 (2004).
[26] A. Retzker and M. Plenio, New J. Phys. **9**, 279 (2007).
[27] J. Cerrillo, A. Retzker, and M. B. Plenio, Phys. Rev. Lett. **104**, 043003 (2010).
[28] A. Albrecht, A. Retzker, C. Wunderlich, and M. B. Plenio, New J. Phys. **13**, 033009 (2011).
[29] S. Zhang, C.-W. Wu, and P.-X. Chen, Phys. Rev. A **85**, 053420 (2012).
[30] Z. Yi, G.-X. Li, and Y.-P. Yang, Phys. Rev. A **87**, 053408 (2013).
[31] S. Zhang, Q.-H. Duan, C. Guo, C.-W. Wu, W. Wu, and P.-X. Chen, Phys. Rev. A **89**, 013402 (2014).
[32] Y. Lu, J.-Q. Zhang, J.-M. Cui, D.-Y. Cao, S. Zhang, Y.-F. Huang, C.-F. Li, and G.-C. Guo, Phys. Rev. A **92**, 023420 (2015).
[33] Z. Yi and W.-j. Gu, Opt. Express **25**, 1314 (2017).
[34] J. Cerrillo, A. Retzker, and M. B. Plenio, Phys. Rev. A **98**, 013423 (2018).
[35] V. Steixner, P. Rabl, and P. Zoller, Phys. Rev. A **72**, 043826 (2005).
[36] P. Rabl, V. Steixner, and P. Zoller, Phys. Rev. A **72**, 043823 (2005).
[37] P. Bushev, D. Rotter, A. Wilson, F. Dubin, C. Becher, J. Eschner, R. Blatt, V. Steixner, P. Rabl, and P. Zoller, Phys. Rev. Lett. **96**, 043003 (2006).
[38] S. Zhang, W. Wu, C.-W. Wu, F.-G. Li, T. Li, X. Wang, and W.-S. Bao, Chin. Phys. B **26**, 074205 (2017).
[39] C. F. Roos, D. Leibfried, A. Mundt, F. Schmidt-Kaler, J. Eschner, and R. Blatt, Phys. Rev. Lett. **85**, 5547 (2000).

[40] Y. Lin, J. P. Gaebler, T. R. Tan, R. Bowler, J. D. Jost, D. Leibfried, and D. J. Wineland, Phys. Rev. Lett. **110**, 153002 (2013).
[41] T. Kampschulte, W. Alt, S. Manz, M. Martinez-Dorantes, R. Reimann, S. Yoon, D. Meschede, M. Bienert, and G. Morigi, Phys. Rev. A **89**, 033404 (2014).
[42] R. Lechner, C. Maier, C. Hempel, P. Jurcevic, B. P. Lanyon, T. Monz, M. Brownnutt, R. Blatt, and C. F. Roos, Phys. Rev. A **93**, 053401 (2016).
[43] N. Scharnhorst, J. Cerrillo, J. Kramer, I. D. Leroux, J. B. Wübbena, A. Retzker, and P. O. Schmidt, Phys. Rev. A **98**, 023424 (2018).
[44] E. Jordan, K. A. Gilmore, A. Shankar, A. Safavi-Naini, J. G. Bohnet, M. J. Holland, and J. J. Bollinger, Phys. Rev. Lett. **122**, 053603 (2019).
[45] L. Feng, W. L. Tan, A. De, A. Menon, A. Chu, G. Pagano, and C. Monroe, Phys. Rev. Lett. **125**, 053001 (2020).
[46] M. Qiao, Y. Wang, Z. Cai, B. Du, P. Wang, C. Luan, W. Chen, H.-R. Noh, and K. Kim, Phys. Rev. Lett. **126**, 023604 (2021).
[47] C. Huang, S. Chai, and S.-Y. Lan, Phys. Rev. A **103**, 013305 (2021).
[48] S. Zhang, J.-Q. Zhang, W. Wu, W.-S. Bao, and C. Guo, New J. Phys. **23**, 023018 (2021).
[49] X.-Q. Li, S. Zhang, J. Zhang, W. Wu, C. Guo, and P.-X. Chen, arXiv:2106.05443.
[50] J. I. Cirac, R. Blatt, P. Zoller, and W. D. Phillips, Phys. Rev. A **46**, 2668 (1992).
[51] V. Gorini, A. Kossakowski, and E. C. G. Sudarshan, J. Math. Phys. **17**, 821 (1976).
[52] G. Lindblad, Commun. Math. Phys. **48**, 119 (1976).
[53] G. Morigi, Phys. Rev. A **67**, 033402 (2003).
[54] M. Roghani and H. Helm, Phys. Rev. A **77**, 043418 (2008).
[55] J. R. Johansson, P. D. Nation, and F. Nori, Comput. Phys. Commun. **183**, 1760 (2012).